

WestminsterResearch

<http://www.westminster.ac.uk/westminsterresearch>

Ligand-specific conformational change of the G-protein-coupled receptor ALX/FPR2 determines proresolving functional responses

Cooray SN, Gobbetti T, Montero-Melendez T, McArthur S, Thompson D, Clark AJL, Flower RJ and Perretti M

This is a copy of the final publisher version of a journal article published in Proceedings of the National Academy of Sciences, 2013 Nov 5;110(45):18232-7. doi: 10.1073/pnas.1308253110. Epub 2013 Oct 9. It is available online at:

<http://dx.doi.org/10.1073/pnas.1308253110>

Freely available online through the PNAS open access option.

The WestminsterResearch online digital archive at the University of Westminster aims to make the research output of the University available to a wider audience. Copyright and Moral Rights remain with the authors and/or copyright owners.

Whilst further distribution of specific materials from within this archive is forbidden, you may freely distribute the URL of WestminsterResearch: (<http://westminsterresearch.wmin.ac.uk/>).

In case of abuse or copyright appearing without permission e-mail repository@westminster.ac.uk

Ligand-specific conformational change of the G-protein-coupled receptor ALX/FPR2 determines proresolving functional responses

Sadani N. Cooray^a, Thomas Gobetti^a, Trinidad Montero-Melendez^a, Simon McArthur^a, Dawn Thompson^a, Adrian J. L. Clark^b, Roderick J. Flower^a, and Mauro Perretti^{a,1}

^aWilliam Harvey Research Institute, Barts and The London School of Medicine, London EC1M 6BQ, United Kingdom; and ^bSt. George's University of London, London SW17 0RE, United Kingdom

Edited by Charles N. Serhan, Brigham and Women's Hospital/Harvard Medical School, Boston, MA, and accepted by the Editorial Board September 10, 2013 (received for review May 3, 2013)

Formyl-peptide receptor type 2 (FPR2), also called ALX (the lipoxin A4 receptor), conveys the proresolving properties of lipoxin A4 and annexin A1 (AnxA1) and the proinflammatory signals elicited by serum amyloid protein A and cathelicidins, among others. We tested here the hypothesis that ALX might exist as homo- or heterodimer with FPR1 or FPR3 (the two other family members) and operate in a ligand-biased fashion. Coimmunoprecipitation and bioluminescence resonance energy transfer assays with transfected HEK293 cells revealed constitutive dimerization of the receptors; significantly, AnxA1, but not serum amyloid protein A, could activate ALX homodimers. A p38/MAPK-activated protein kinase/heat shock protein 27 signaling signature was unveiled after AnxA1 application, leading to generation of IL-10, as measured in vitro (in primary monocytes) and in vivo (after i.p. injection in the mouse). The latter response was absent in mice lacking the ALX ortholog. Using a similar approach, ALX/FPR1 heterodimerization evoked using the panagonist peptide Ac2-26, identified a JNK-mediated proapoptotic path that was confirmed in primary neutrophils. These findings provide a molecular mechanism that accounts for the dual nature of ALX and indicate that agonist binding and dimerization state contribute to the conformational landscape of FPRs.

inflammation | leukocyte | resolution signaling

G-protein-coupled receptors (GPCRs) constitute a large family of cell surface receptors that share structural characteristics and perform pivotal biological functions, transducing signals from hormones, autacoids, and chemokines. The human GPCR termed “ALX/FPR2” (formyl peptide receptor type 2 or lipoxin A₄ receptor, hereafter referred to as “ALX”) is a unique GPCR, shown to convey signals induced by proteins, peptides, and lipid ligands (1). ALX belongs to a small family of receptors that is also activated by formylated peptides, short amino acid sequences with an N-terminal formyl group released by pathogenic and commensal bacteria, as well as by mitochondria upon cell damage. There are three human FPRs and they are termed FPR1, ALX, and FPR3 (2). In view of their different nature and potential engagement with a large number endogenous and exogenous ligands, elucidation of FPR functions may reveal important biological pathways.

ALX is an unconventional receptor for the diversity of its agonists and because it can convey contrasting biological signals. The proresolving and anti-inflammatory properties of the protein annexin A1 (AnxA1) and the lipid lipoxin A₄ (LXA₄), which include neutrophil apoptosis and macrophage efferocytosis, are mediated by this receptor, as shown using pharmacological approaches (1, 3) and more recently with knockout mouse models (4). At the same time, the proinflammatory responses elicited by the cathelicidin-associated antimicrobial peptide LL-37 and serum amyloid protein A (SAA) are also mediated by ALX, which modulates leukocyte activation, recruitment to the site of inflammation, and lifespan (5–7). Moreover, LXA₄ and

AnxA1 engage ALX to favor a macrophage M2 phenotype, whereas LL-37 and SAA used the same receptor to induce an M1 phenotype (8). In a similar vein using human neutrophils, nanomolar concentrations of LXA₄ counteracted LL-37-mediated release of leukotriene B₄, both actions being conveyed by ALX (9).

Using resonance energy transfer (RET) techniques to investigate GPCR interactions, a number of studies reported agonist stimulation to initiate dimerization between certain GPCRs, which may otherwise exist as monomeric structures (10) or that agonists enhance the interaction between preformed dimers (11). Agonist-induced changes in RET signal could be attributed to conformational changes occurring within the receptor in response to agonist binding (12). Finally, activation of downstream signaling pathways may also influence conformational changes within the receptors (13, 14). We tested here whether the ability of ALX to transduce the bioactions elicited by distinct agonists is modulated by conformational changes.

Results

Homo-/Heterodimerization of FPR1 with ALX and FPR3 Is Enhanced by a Panagonist Peptide. HEK293 cells were used for a transfection-based approach to investigate the potential homo-/

Significance

Inflammation is a crucial host defense response but can cause chronic disease if unregulated. Several endogenous anti-inflammatory and proresolving circuits balance and modulate inflammation, including a mechanism centered on the formyl peptide receptor (FPR) family. One receptor, ALX/FPR2, recognizes both proinflammatory and proresolving signals. We have investigated this unusual molecular mechanism finding that anti-inflammatory, but not proinflammatory signals, activate homodimers of this receptor. This triggers intracellular changes culminating in the release of anti-inflammatory mediators such as IL-10. Heterodimers of ALX with other FPR receptors can transduce proapoptotic signals. These results explain how both the development and resolution of inflammation may be integrated by the same receptor system and show how drugs can be developed that have only anti-inflammatory effects.

Author contributions: S.N.C., T.M.-M., A.J.L.C., R.J.F., and M.P. designed research; S.N.C., T.G., T.M.-M., S.M., and D.T. performed research; S.N.C., T.G., T.M.-M., S.M., D.T., A.J.L.C., R.J.F., and M.P. analyzed data; and S.N.C. and M.P. wrote the paper.

The authors declare no conflict of interest.

This article is a PNAS Direct Submission. C.N.S. is a guest editor invited by the Editorial Board.

Freely available online through the PNAS open access option.

See Commentary on page 18033.

¹To whom correspondence should be addressed. E-mail: m.perretti@qmul.ac.uk.

This article contains supporting information online at www.pnas.org/lookup/suppl/doi:10.1073/pnas.1308253110/-DCSupplemental.

heterodimerization between FPRs and chosen because they do not express any of the three receptors (Fig. S1A). Initial analyses determined that the epitope-tagged constructs were properly expressed on the cell surface 24 h posttransfection (Fig. S1B and C). Colocalization between the FPR1 and ALX at the cell surface was observed (Fig. 1A). To monitor physical interaction between the receptors, HEK293 cells were transfected with FPR1 × 3Flag construct along with either FPR1 × 3HA, ALX × 3HA or FPR3 × 3HA constructs for immunoprecipitation (IP) with

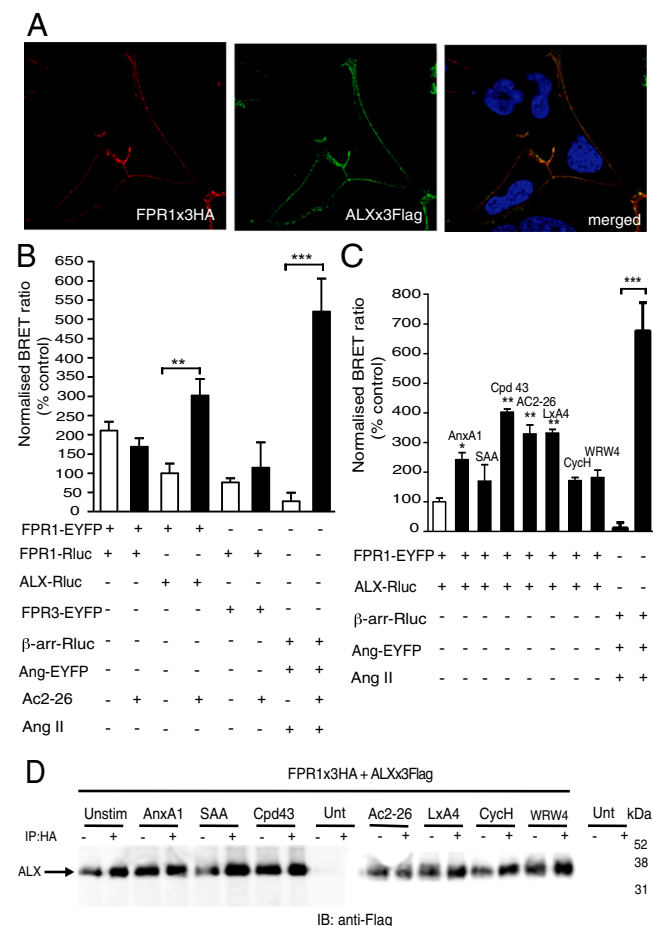


Fig. 1. Expression and dynamics of FPR1 in transfected HEK293 cells. (A) HEK293 cells were transfected with HA-FPR1 (red) and Flag-ALX (green); receptor colocalization shown in the merged image (yellow). Data representative of three analyses conducted with different cell preparations. (B) FPR1 homodimerization and heterodimerization with ALX and FPR3 using BRET. HEK293 cells transfected with FPR1-EYFP and FPR1-Rluc, FPR1-EYFP and ALX-Rluc, or FPR1-Rluc and FPR3-EYFP constructs were stimulated with Ac2-26 (10^{-5} M) for 10 min. Data (mean \pm SEM of three experiments) are calculated against unstimulated ALX/FPR1 values. $**P < 0.01$, $***P < 0.001$ vs. control (FPR1-EYFP/FPR1-Rluc cells). (C) FPR1/ALX heterodimerization. FPR1-EYFP and ALX-Rluc were coexpressed in HEK293 cells and, after 24 h, incubated with AnxA1 (10^{-8} M), SAA (10^{-7} M), compound 43 (Cpd43; 10^{-6} M), Ac2-26 (10^{-5} M), LXA₄ (10^{-7} M), cyclosporin H (CycH; 10^{-5} M), or WRW4 (10^{-5} M) for 10 min. As positive controls for the assays, cells were transfected with β -arrestin-Rluc and angiotensin II receptor type 1 (AT1R)-EYFP constructs and stimulated with angiotensin II (AngII; 10^{-6} M) for 10 min. Data are mean \pm SEM of three experiments in triplicate. $*P < 0.05$, $**P < 0.01$ vs. control (FPR1-EYFP and ALX-Rluc cells). $***P < 0.001$ for AngII-treated cells vs. respective control. (D) Heterodimerization between FPR1 and ALX. FPR1 \times 3HA and ALX \times 3Flag-transfected HEK293 cells were stimulated with the indicated agonists as in B. Immunoprecipitation of FPR1 \times 3HA with HA agarose beads coprecipitated ALX \times 3Flag as determined by immunoblotting with anti-Flag antibody. Blots are representative of three independent experiments.

an anti-HA antibody. Using this protocol, we observed that FPR1 can constitutively homodimerize and heterodimerize with ALX and FPR3 (Fig. S1D). This effect was not modified by addition of the panagonist peptide Ac2-26 [annexin A1 N terminal peptide Ac2-26 (acetyl-AMVSEFLKQAWIENEE-QEYVVQTVK)] (15). Next, we used the bioluminescence RET (BRET) technique to explore receptor interaction in living cells.

HEK293 cells transfected with FPR1-enhanced YFP (EYFP) and FPR1-Renilla luciferase (Rluc), FPR1-EYFP and ALX-Rluc, or FPR1-Rluc and FPR3-EYFP constructs showed an interaction between these receptors as determined by detection of BRET signal in absence of agonist application. Addition of peptide Ac2-26 (10^{-5} M), although not affecting the BRET signal between FPR1 homodimers or FPR1-FPR3 heterodimers, produced a significant enhancing effect on FPR1-ALX heterodimer signal (Fig. 1B). To rule out the possibility of nonspecific interactions, we investigated whether the FPR1 and ALX receptors could form heterodimers with another class A GPCR, namely, the angiotensin 1 receptor. These receptors did not interact, nor was a signal obtained upon addition of the respective agonists Ac2-26 or angiotensin II, as determined by BRET and co-IP techniques (Fig. S2).

We then focused on the interaction between the FPR1 and ALX. The anti-inflammatory agonists AnxA1 (10^{-8} M), peptide Ac2-26 (10^{-5} M), and LXA₄ (10^{-7} M), together with the small molecule compound 43 (Cpd43; 10^{-6} M), produced a significant enhancement in BRET signal (Fig. 1C). Complete physical validation of the LXA₄ agonist was carried out using liquid chromatography-tandem mass spectrometry (LC-MS-MS) and UV, with spectra and profiles matching those reported earlier (Fig. S3) (16). The BRET response was not obtained with SAA (10^{-7} M) or the selective FPR1 or ALX antagonists (cyclosporin H and WRW4, respectively) (Fig. 1C). In line with FPR1 dimerization (Fig. S1D), addition of these ligands did not enhance the co-IP between FPR1 and ALX (Fig. 1D). The central role seemingly played by ALX in the observed agonist-specific conformational changes prompted us to test homodimerization responses.

Contrasting Effect of AnxA1 and SAA on ALX Homodimerization. Homodimerization of ALX was investigated with ALX \times 3Flag and ALX \times 3HA constructs, followed by IP with anti-HA and immunoblotting with anti-Flag antibody. Addition of AnxA1 (10^{-8} M), Ac2-26 (10^{-5} M), or SAA (10^{-7} M) did not influence receptor dimerization, and a band corresponding to the correct molecular weight for an ALX dimer was observed (Fig. 2A). ALX dimerization was investigated in living cells following transfection with ALX-Rluc and ALX-EYFP constructs. At 24 h posttransfection, cells were stimulated with AnxA1 (10^{-8} M), Ac2-26 (10^{-5} M), or SAA (10^{-7} M) for 10 min. As was seen with the FPR1-ALX heterodimer (Fig. 1), peptide Ac2-26 produced an enhanced BRET signal (Fig. 2B). ALX anti-inflammatory and proinflammatory ligands displayed opposite effects: AnxA1 enhanced, whereas SAA decreased, the BRET signal (Fig. 2B). At 10^{-9} M, AnxA1 elicited a similar BRET signal (2.2 ± 0.4 -fold increase over basal; $n = 3$). Representative real-time BRET analysis plots display single-order kinetics in response to Ac2-26 and AnxA1, but not SAA (Fig. 2C). Tested at 10^{-7} M, LXA₄ enhanced the BRET signal between ALX homodimers (Fig. S4A). Of interest, this bioactive lipid did not interfere with the BRET signal provoked by AnxA1. SAA, over a wide range of concentrations (up to 3×10^{-6} M), failed to incite a BRET response (Fig. S4B); however, it attenuated the enhancement in BRET signal provoked by AnxA1 (Fig. S4A). Collectively, these results shed some light into the conflicting behavior imposed on ALX by functionally different agonists, indicating, presumably, differential activation of distinct downstream signaling pathways.

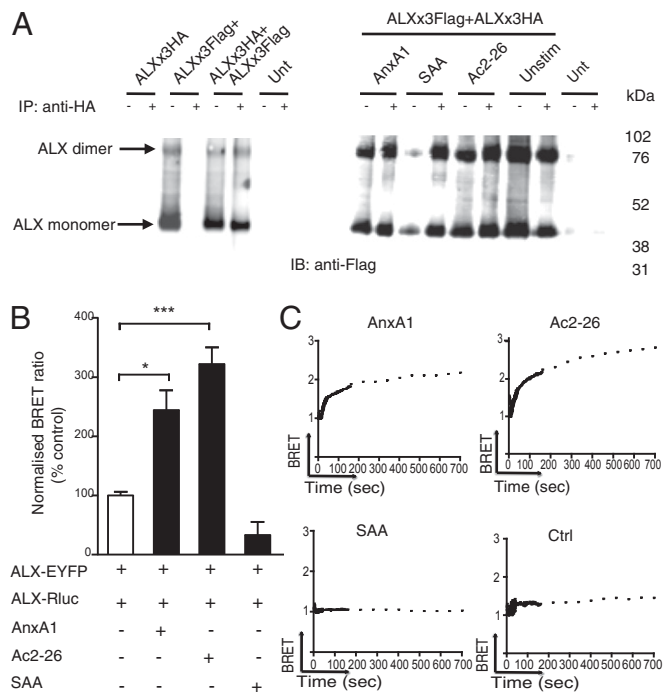


Fig. 2. Agonist-induced ALX homodimerization. (A) Homodimerization of ALX as demonstrated using co-IP. HEK293 cells were transfected with either ALX x 3Flag, ALX x 3HA, or both ALX x 3Flag and ALX x 3HA constructs. Twenty-four hours later, cells were stimulated with AnxA1 (10^{-8} M), SAA (10^{-7} M), or Ac2-26 (10^{-5} M) for 10 min. Immunoprecipitation of ALX x 3HA using anti-HA agarose beads coprecipitated ALX x 3Flag as determined by immunoblotting with anti-Flag antibody. Blots are representative of three experiments. (B) Homodimerization of ALX using BRET. HEK293 cells, transfected with ALX-Rluc and ALX-EYFP, were stimulated with the indicated agonists as in A. Data (mean \pm SEM of three experiments) calculated against basal ALX/ALX values. * $P < 0.05$, *** $P < 0.001$ vs. vehicle-treated cells (white bar). (C) Examples of real-time BRET analysis between ALX-Rluc and ALX-EYFP expressing HEK293 cells upon application of vehicle (Ctrl), AnxA1 (10^{-8} M), Ac2-26 (10^{-5} M), or SAA (10^{-7} M), as monitored for up to 12 min.

Definition of a Specific Signaling Pathway Activated by the AnxA1/ALX Interaction. Initially we established that ALX functioned normally in that Cpd43, SAA, and AnxA1 provoked dephosphorylation of moesin in HEK293 cells transfected with ALX (Fig. S5). We then attempted to elucidate unique signaling pathways using a human proteome profiler MAPK assay (SI Materials and Methods). Upon addition of AnxA1 (10^{-8} M) or SAA (10^{-7} M) onto HEK293 cells transfected with ALX, differences in a number of signaling molecules emerged (Figs. S6 and S7). Close analysis indicated potential engagement by AnxA1 of a unique pathway, onto which we focused the next series of experiments.

Addition of AnxA1 to ALX-HEK293 cells provoked downstream phosphorylation of p38, MAPK-activated protein kinase (MAPKAPK), and the small heat-shock protein Hsp27 (Fig. S6B) as assessed by Western blotting. Importantly, these data were confirmed in nontransfected human monocytic U937 cells (Fig. 3A), which constitutively express ALX (Fig. S14), and human primary monocytes (Fig. 3A), which also express ALX (2). In Fig. 3A (bar graph) we report the cumulative data of four experiments conducted with primary monocytes, showing that AnxA1, but not SAA, can induce phospho-Hsp27. AnxA1 phosphorylated Hsp27 in a concentration-dependent fashion, with higher efficacy at 10^{-7} M (Fig. S8A). Like SAA, the proinflammatory ALX agonist LL-37 was unable to phosphorylate Hsp27 at any concentrations tested (Fig. S8 B and C). Finally, we established that phosphorylation of MAPKAPK2

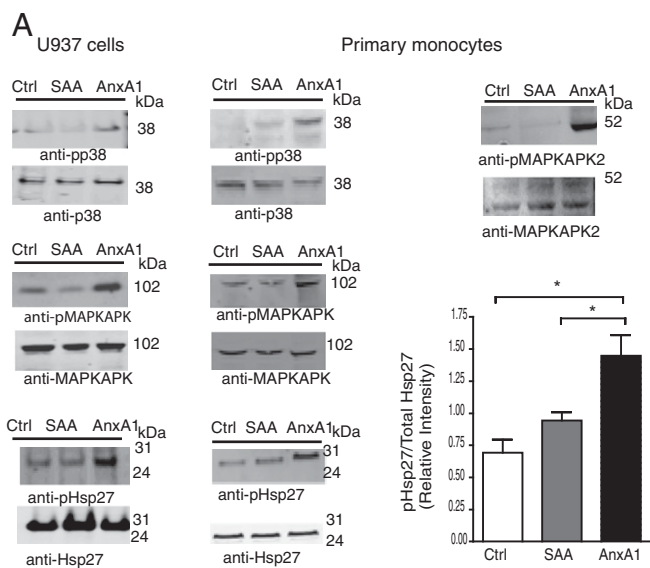


Fig. 3. AnxA1/ALX proresolving signaling signature leads to IL-10 release. (A) U937 cells (1×10^6) or human primary monocytes (5×10^5) were treated for 10 min with vehicle (Ctrl), AnxA1 (10^{-8} M) or SAA (10^{-7} M) and lysates subjected to Western blotting against phosphorylated and unphosphorylated p38, MAPKAPK1, MAPKAPK2, and Hsp27 (representative of three experiments). The cumulative data for Hsp27 are shown in bar graph ($n = 3$ distinct preparations). (B) Schema of the p38/MAPKAPK/Hsp27/IL-10 pathway. Human monocytes (1×10^6) were treated with AnxA1 (10^{-8} M) for 6 h, with or without pretreatment with the p38 inhibitor SB203580 (10^{-7} M, 10 min). Data are mean \pm SEM, three donors assayed in duplicate. ** $P < 0.01$ vs. Ctrl, +++ $P < 0.001$ vs. AnxA1 alone. (C) AnxA1 (1 μ g) or saline (200 μ L) were injected i.p. into wild-type or Alx-Fpr2/3 knockout (KO) mice and peritoneal lavages were harvested 6 h later. Data are mean \pm SEM of six mice per group. * $P < 0.05$ vs. respective wild type. (D) Mice were treated with 10 mg/kg i.p. LPS and IL-10 levels were measured at the 24-h time point. (Inset) Endogenous AnxA1 levels in lavage fluids. Data are mean \pm SEM of six mice per group. * $P < 0.05$ vs. wild type.

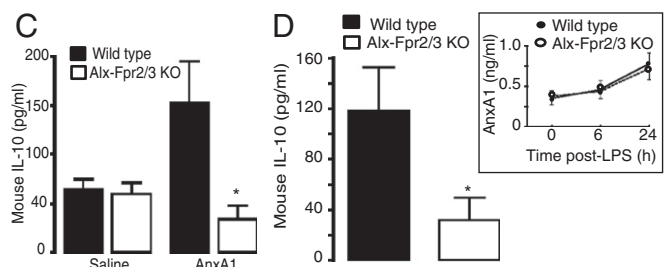


Fig. 3. AnxA1/ALX proresolving signaling signature leads to IL-10 release. (A) U937 cells (1×10^6) or human primary monocytes (5×10^5) were treated for 10 min with vehicle (Ctrl), AnxA1 (10^{-8} M) or SAA (10^{-7} M) and lysates subjected to Western blotting against phosphorylated and unphosphorylated p38, MAPKAPK1, MAPKAPK2, and Hsp27 (representative of three experiments). The cumulative data for Hsp27 are shown in bar graph ($n = 3$ distinct preparations). (B) Schema of the p38/MAPKAPK/Hsp27/IL-10 pathway. Human monocytes (1×10^6) were treated with AnxA1 (10^{-8} M) for 6 h, with or without pretreatment with the p38 inhibitor SB203580 (10^{-7} M, 10 min). Data are mean \pm SEM, three donors assayed in duplicate. ** $P < 0.01$ vs. Ctrl, +++ $P < 0.001$ vs. AnxA1 alone. (C) AnxA1 (1 μ g) or saline (200 μ L) were injected i.p. into wild-type or Alx-Fpr2/3 knockout (KO) mice and peritoneal lavages were harvested 6 h later. Data are mean \pm SEM of six mice per group. * $P < 0.05$ vs. respective wild type. (D) Mice were treated with 10 mg/kg i.p. LPS and IL-10 levels were measured at the 24-h time point. (Inset) Endogenous AnxA1 levels in lavage fluids. Data are mean \pm SEM of six mice per group. * $P < 0.05$ vs. wild type.

[the kinase upstream of Hsp27 (17, 18) and not present in the proteome profiler] was occurring in human primary monocytes (Fig. 3A). Collectively, these results indicate that the p38/MAPKAPK/Hsp27 pathway is a genuine response evoked by AnxA1, and not SAA, upon activation of ALX.

It was important to corroborate these results in a functional manner. In monocytes, the p38/MAPKAPK/Hsp27 pathway is associated with IL-10 generation (Fig. 3B, schema). Stimulation of isolated monocytes with AnxA1 (10^{-8} M; 6 h) induced a significant release of IL-10 that was abolished by pretreatment of cells with the p38 inhibitor SB203580 (Fig. 3B). Importantly, this effect could be replicated in vivo, where i.p. injection of an anti-inflammatory dose of the protein (1- μ g equivalent to 27 pmol) elicited a threefold increase in IL-10 (Fig. 3C). The effect was absent in Alx-Fpr2/3 KO mice. Then we established the relevance of this pathway in more complex settings. By 24 h post-LPS, a marked accumulation of IL-10 had occurred in wild-type but not Alx-Fpr2/3 KO mice (Fig. 3D). This was not due to differences in the release of endogenous AnxA1 (similar between genotypes; Fig. 3D, *Inset*).

Characterization of FPR1 and ALX Heterodimerization. Finally, we used a proteome profiler to investigate the effect of the pan-agonist Ac2-26 on HEK293 cells transfected with FPR1, ALX, or cotransfected with both receptors. A clear difference in signaling transfected HEK293 cells expressing either FPR1 or ALX, or cells coexpressing FPR1 and ALX, was detected (Fig. 4A and Fig. S9). Analysis of the single transfections indicated that the ALX response was stronger than that observed with FPR1; however, the most pronounced activation was observed upon coexpression of both FPR1 and ALX, which showed a selective activation of the JNK pathway (Fig. 4A, *Lower*). Proteome data

were confirmed by Western blotting analyses for phospho-ERK and phospho-JNK in HEK293 cells (Fig. 4B, *Top* and *Middle*) as well as in primary neutrophils (shown only for phospho-JNK; Fig. 4B, *Bottom*).

The JNK pathway has been linked to cell apoptosis (19), a process AnxA1 promotes in human neutrophils (20). Of note, this leukocyte type expresses FPR1 and ALX, but not FPR3 (2), making it ideal to explore heterodimerization in primary cells. We conducted functional experiments using protocols validated for LXA₄: this ALX agonist abolishes the delay in apoptosis of SAA-treated neutrophils (7). In line with these studies, addition of SAA augmented neutrophil lifespan with a significant effect at >6 h (Fig. 5A). Peptide Ac2-26 counteracted this survival signal and was effective in augmenting the degree of both early and late apoptosis. Addition of the JNK inhibitor SP600125 abolished the effect of peptide Ac2-26 (Fig. 5B). We substantiated these results at the molecular level by monitoring caspase-3 activation. Addition of peptide Ac2-26 to SAA-treated neutrophils resulted in caspase-3 cleavage (an effect not visible with SAA alone) and this was prevented by the JNK inhibitor SP600125 (Fig. 5C).

Discussion

The human FPR termed ALX can elicit opposing responses such as cell survival vs. death, cell activation vs. inhibition, and in vivo pro- and anti-inflammatory effects. Here we investigated whether ALX could dimerize and if this conformational event could account for these biological functions. Using transfected systems, we found a significant change in the BRET signal detected between the FPR1/ALX heterodimer and ALX/ALX homodimer in response to proresolving ALX agonists.

Compared with FPR1 and FPR3 in these experiments, ALX displayed higher propensity to elicit a BRET signal in response to agonist stimulation. This feature was shared by distinct proresolving and anti-inflammatory agonists, but not by the proinflammatory agonist SAA. Thus, it is plausible that agonist-biased ALX dimerization can distinguish between agonists endowed with distinct, somewhat opposing biological properties. Because addition of ALX antagonists, which bind but do not activate the receptor, did not result in a significant change in BRET signal, we propose that the conformational change of ALX produced by AnxA1, Ac2-26, LXA₄, and Cpd43 was not merely due to ligand-receptor interaction. These conclusions are substantiated by analogous observations reported for the β_2 -adrenergic receptor (21).

Our molecular analyses confirmed that ALX homo- and heterodimerization yielded specific signaling profiles. The canonical G_i-linked GPCR signaling was confirmed by detection of ERK phosphorylation and moesin dephosphorylation, both well-characterized readouts of downstream ALX activation (22), but noteworthy connections were also unveiled. Qualitative results obtained with the profiler were supported by Western blotting analysis, using the strategy of rapidly translating data obtained with transfected cells to primary leukocytes. In this manner, we could define a “specific” ALX/ALX dimer signature activated by AnxA1, but not by SAA or LL-37, which is the p38/MAPKAPK/Hsp27/IL-10 pathway. Hsp27 is a chaperone protein (for review, ref. 23) endowed with immunomodulatory and anti-inflammatory actions, including the release of IL-10 (24).

It is noteworthy that, whereas LXA₄ did not affect the ALX conformational change promoted by AnxA1, SAA did reduce this response, thus providing a molecular explanation for the antagonistic properties of SAA and AnxA1 (25).

AnxA1 addition to cells in vitro augmented IL-10 production in a p38-mediated fashion. In vivo injections of anti-inflammatory doses of AnxA1 (26) led to IL-10 production in an ALX-dependent manner, as demonstrated using a mouse colony deficient in the ortholog for the human receptor (4). Some evidence for a link between AnxA1 and IL-10 has been advanced in the literature using macrophages (27) and in models of gut injury (28).

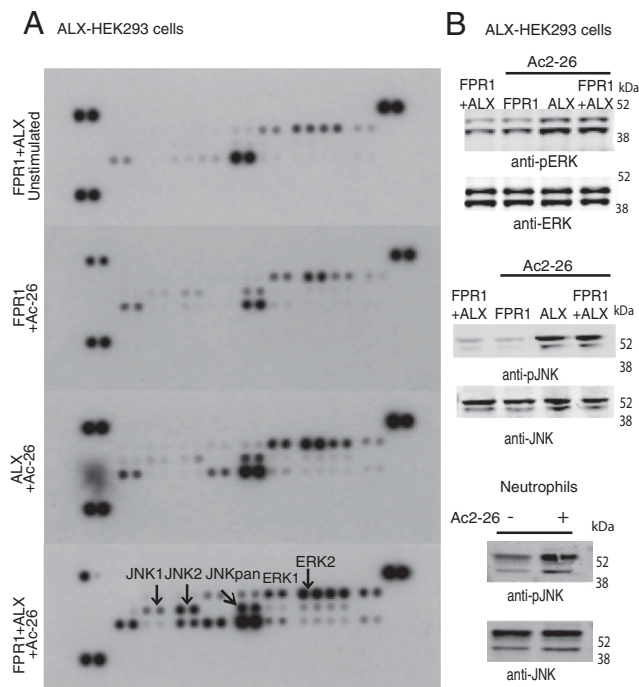


Fig. 4. Identification of an ALX/FPR1 signaling signature. (A) Proteome profiler array on HEK293 cells transfected with FPR1, ALX, or both FPR1 and ALX, before 10-min stimulation with Ac2-26 (10^{-5} M). Control cells were left unstimulated. (B) Western blotting analysis on HEK293 cells (1×10^6) transfected with human FPR1, ALX, or FPR1 + ALX to assess the phosphorylation status of ERK and JNK (*Top* and *Middle*). Jnk phosphorylation in neutrophils stimulated with Ac2-26 for 10 min (*Bottom*). Blots are representative of three individual experiments.

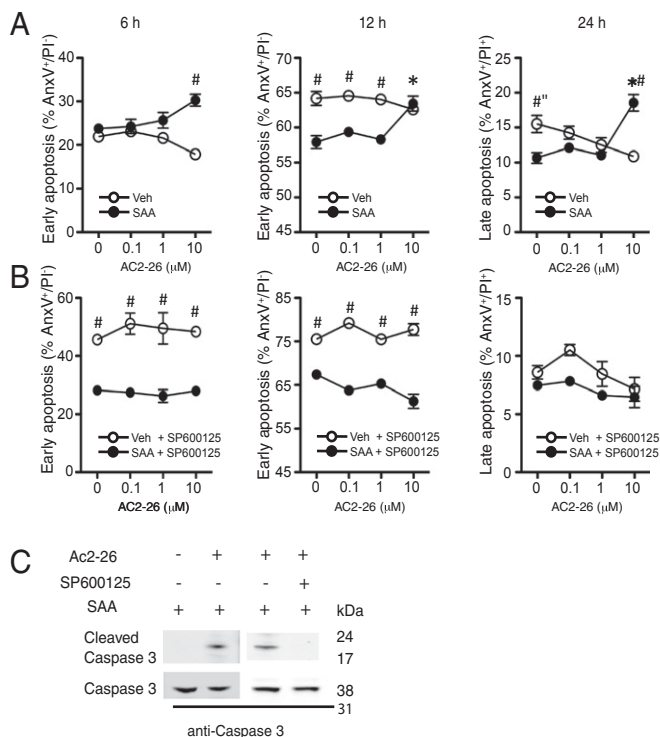


Fig. 5. Peptide Ac2-26 rescues the antiapoptotic effect of SAA. (A and B) Human neutrophils (1×10^6) were incubated with SAA ($10 \mu\text{g/mL}$) alone or with Ac2-26 (10^{-5} M), before assessment of early (6–12 h) and late (24 h) apoptosis by flow cytometry (AnxAV-FITC/PI double staining). Experiments were run in the absence (A) or presence (B) of the JNK inhibitor SP600125 ($2 \times 10^{-6} \text{ M}$) added to cells 30 min before. Data are mean \pm SEM, $n = 3$ independent donors. * $P < 0.05$ one-way ANOVA (Ac2-26 vs. 0 concentration); # $P < 0.05$ two-way ANOVA (vehicle vs. SAA). (C) Western blotting for caspase-3 cleavage in human neutrophils treated with SAA alone or together with Ac2-26 (10^{-5} M) for 24 h in the presence or absence of SP600125 ($2 \times 10^{-6} \text{ M}$). Blot representative of three experiments.

Our data provide molecular support to this pathway, linking the protein AnxA1—a master regulator of resolution (29)—and the cytokine IL-10 to ALX homodimerization. The experiments conducted with LPS indicated that activation of endogenous ALX may be pivotal for the generation of IL-10, a hypothesis that needs to be extended to more complex disease models.

We concluded the study by applying the same experimental approach to define the signaling signature of the FPR1/ALX heterodimer. These chimeric analyses indicated that ALX is more active than FPR1 for phosphosignaling with transfected cells, and that cotransfection followed by agonist application elicited a strong JNK response, absent in cells transfected with just a single receptor. In this set of experiments, we focused on potential candidates for the apoptosis pathway: AnxA1 and its peptide Ac2-26, which derives from the N-terminal region of the protein and may be generated in vivo in inflammatory exudates, promote neutrophil apoptosis in vitro (20) and in vivo (30). Relevantly, FPR1 and ALX, but not FPR3, are expressed on human and mouse neutrophils (2); hence, these cells could be used in the absence of the potential confounding presence of FPR3. The results obtained with the transfected HEK293 cell model were therefore validated with primary neutrophils.

Filép and coworkers have described the ability of LXA₄ to override the effects of SAA, a prosurvival factor for human neutrophils (7). Fine tuning of neutrophil lifespan is fundamental for an appropriate inflammatory reaction, avoiding the risk for chronicity (31, 32). The ability of peptide Ac2-26 to affect neutrophil

lifespan was abrogated in the presence of JNK inhibition, providing a functional link to the post-ALX/FPR1 dimerization signaling events. Supporting these unique data are the association of JNK in both extrinsic and intrinsic apoptotic pathways (19).

The signaling signature afforded by the ALX/ALX and ALX/FPR1 dimerization can be exploited to infer specific engagement of ALX by proresolving ligands in diseased cells and tissues, using the p38/MAPKAPK/Hsp27/IL-10 and JNK/caspase-3 pathways as readouts. For instance, we now have the tools to establish whether ALX/ALX formation failed, or was not favored, in cells of patients suffering from a given vascular pathology, perhaps explaining the ineffective up-regulation of protective ligands such as AnxA1 or LXA₄ (33). These findings are of wide impact because ALX is emerging as an important regulatory receptor in several distinct human pathologies, ranging from rheumatoid synovitis (34) to human colitis tissue (35), from ischemic damage (36) to asthma (37). A detailed understanding of the importance of dimerization evoked by proresolving agonists AnxA1 and LXA₄ to ALX biology will clarify the impact of this receptor on the therapeutic control of pathogenic states. For instance, this conformational alteration of ALX may be relevant for the proresolving properties of resolvin D1 as described in models of colitis (38). Finally, our unique data can guide the development of synthetic ALX agonists, including stable LXA₄ analogs (39), peptide mimetics (40), or small molecules (41), with the ultimate goal of developing innovative therapeutics to moderate overexuberant inflammatory responses.

Materials and Methods

SI Materials and Methods provides an extended version of the experimental procedures and details of reagents.

Plasmid Constructions, Cell Culture, and Transfections. FPR1-Rluc, ALX-Rluc, and FPR3-Rluc were generated by subcloning human FPR1, ALX, and FPR3 into the codon humanized *Renilla* luciferase vectors pRLuc N1 and pRLuc C3. FPR1 and ALX were cloned into pEYFP-N1 to produce FPR1-EYFP and ALX-EYFP. FPR1 and ALX were cloned into p3 × Flag-CMV-14 to produce FPR1 × 3Flag and ALX × 3Flag. FPR1 × 3HA, ALX × 3HA and FPR3 × 3HA were purchased from Missouri S&T cDNA Resource Center (www.cDNA.org). HEK293A cells were transfected with Lipofectamine.

Reverse Transcriptase PCR. Total RNA was extracted from HEK293 cells and U937 cells, and cDNA was synthesized for PCR analysis using ALX-specific primer pairs.

Fluorescence-Associated Cell Sorting and Confocal Microscopy Analyses. HEK293 cells were transfected with x3HA-tagged FPRs and stained with anti-HA antibodies prior to flow cytometry analysis. For colocalization, cells were cotransfected with HA-tagged FPR1 and FLAG-tagged ALX and, 24 h later, incubated with anti-FLAG M1 and anti-HA antibody (Sigma). Cells were fixed with formaldehyde, permeabilized, and stained with secondary antibody. Coverslips were mounted and visualized using a Zeiss LSM confocal microscope (Carl Zeiss).

BRET Assay in Living Cells. HEK293 cells were transfected and 24 h later transferred into 96-well black Optiplates (Perkin-Elmer). For end-point assays, cells were stimulated with ligands for 10 min. Coelenterazine-h (Invitrogen) was added to a final concentration of $5 \mu\text{M}$ and readings were collected (Polarstar Omega plate reader). For real-time experiments, coelenterazine-h ($5 \mu\text{M}$) was added before ligand injection. Cells were kept at 37°C throughout. The BRET ratio is defined as emission at 530 nm (light emitted by EYFP)/emission at 485 nm (light emitted by Rluc) (13).

Proteome Profiler Arrays. FPR1, ALX, or FPR1 + ALX transfected HEK293 cells were stimulated with AnxA1 (10^{-8} M), SAA (10^{-7} M), or Ac2-26 (10^{-5} M) with an incubation time of 10 min, using resting cells as control. Protein quantification was performed on lysates using the human phospho-MAPK array kit (R&D Systems).

Isolation of Human Primary Neutrophils and Monocytes. Peripheral blood from healthy donors was collected in 3.2% (wt/vol) sodium citrate solution (1:10). Neutrophils were isolated via density centrifugation on a Histopaque 1119/

1077 gradient. Human primary monocytes were separated using the RosetteSep cell isolation kit (Stem Cell Technologies).

Western Blotting and Coimmunoprecipitations. For dimerization studies, HEK293 cells were transfected with FPR1 \times 3Flag, ALX \times 3HA and/or FPR1 \times 3HA, ALX \times 3HA or FPR3 \times 3HA constructs and, 24 h later, stimulated for 10 min with the agonists. For co-IPs, lysates were incubated with anti-hemagglutinin (HA) agarose beads and incubated at room temperature for another 2 h. SDS loading buffer was added to the samples and subjected to Western blotting using anti-Flag antibody M2 (1:1,000). Secondary antibody IRDye 800CW goat anti-mouse IgG was used at a 1:10,000 dilution and imaged using the LI-COR Odyssey Infrared Image system.

IL-10 Production. Isolated human monocytes (1×10^6) were incubated with AnxA1 (10^{-8} M) in the presence or absence of the p38 inhibitor SB203580 (10^{-7} M; Sigma Aldrich). At 6 h, cell-free supernatants were harvested and used to quantify human IL-10 levels by ELISA.

- Chiang N, et al. (2006) The lipoxin receptor ALX: Potent ligand-specific and stereoselective actions in vivo. *Pharmacol Rev* 58(3):463–487.
- Ye RD, et al. (2009) International Union of Basic and Clinical Pharmacology. LXXIII. Nomenclature for the formyl peptide receptor (FPR) family. *Pharmacol Rev* 61(2): 119–161.
- Serhan CN, Chiang N, Van Dyke TE (2008) Resolving inflammation: Dual anti-inflammatory and pro-resolution lipid mediators. *Nat Rev Immunol* 8(5):349–361.
- Dufton N, et al. (2010) Anti-inflammatory role of the murine formyl-peptide receptor 2: Ligand-specific effects on leukocyte responses and experimental inflammation. *J Immunol* 184(5):2611–2619.
- Soehnlein O, et al. (2008) Neutrophil secretion products pave the way for inflammatory monocytes. *Blood* 112(4):1461–1471.
- He R, Sang H, Ye RD (2003) Serum amyloid A induces IL-8 secretion through a G protein-coupled receptor, FPRL1/LXA4R. *Blood* 101(4):1572–1581.
- El Kebir D, et al. (2007) Aspirin-triggered lipoxins override the apoptosis-delaying action of serum amyloid A in human neutrophils: A novel mechanism for resolution of inflammation. *J Immunol* 179(1):616–622.
- Li Y, et al. (2011) Pleiotropic regulation of macrophage polarization and tumorigenesis by formyl peptide receptor-2. *Oncogene* 30(36):3887–3899.
- Wan M, Godson C, Guiry PJ, Agerberth B, Haeggström JZ (2011) Leukotriene B₄/antimicrobial peptide LL-37 proinflammatory circuits are mediated by BLT1 and FPR2/ALX and are counterregulated by lipoxin A₄ and resolvin E1. *FASEB J* 25(5):1697–1705.
- Rodríguez-Frade JM, et al. (1999) The chemokine monocyte chemoattractant protein-1 induces functional responses through dimerization of its receptor CCR2. *Proc Natl Acad Sci USA* 96(7):3628–3633.
- Angers S, et al. (2000) Detection of beta 2-adrenergic receptor dimerization in living cells using bioluminescence resonance energy transfer (BRET). *Proc Natl Acad Sci USA* 97(7):3684–3689.
- Couturier C, Jockers R (2003) Activation of the leptin receptor by a ligand-induced conformational change of constitutive receptor dimers. *J Biol Chem* 278(29): 26604–26611.
- Cooray SN, Chung TT, Mazhar K, Szidonya L, Clark AJ (2011) Bioluminescence resonance energy transfer reveals the adrenocorticotropin (ACTH)-induced conformational change of the activated ACTH receptor complex in living cells. *Endocrinology* 152(2):495–502.
- Mary S, et al. (2012) Ligands and signaling proteins govern the conformational landscape explored by a G protein-coupled receptor. *Proc Natl Acad Sci USA* 109(21): 8304–8309.
- Ernst S, et al. (2004) An annexin 1 N-terminal peptide activates leukocytes by triggering different members of the formyl peptide receptor family. *J Immunol* 172(12): 7669–7676.
- Clish CB, Levy BD, Chiang N, Tai HH, Serhan CN (2000) Oxidoreductases in lipoxin A₄ metabolic inactivation: A novel role for 15-onoprostaglandin 13-reductase/leukotriene B₄ 12-hydroxydehydrogenase in inflammation. *J Biol Chem* 275(33):25372–25380.
- Foey AD, et al. (1998) Regulation of monocyte IL-10 synthesis by endogenous IL-1 and TNF-alpha: Role of the p38 and p42/44 mitogen-activated protein kinases. *J Immunol* 160(2):920–928.
- Ahlers A, et al. (1994) Interleukin-1-induced intracellular signaling pathways converge in the activation of mitogen-activated protein kinase and mitogen-activated protein kinase-activated protein kinase 2 and the subsequent phosphorylation of the 27-kilodalton heat shock protein in monocytic cells. *Mol Pharmacol* 46(6):1077–1083.
- Cui J, Zhang M, Zhang YQ, Xu ZH (2007) JNK pathway: Diseases and therapeutic potential. *Acta Pharmacol Sin* 28(5):601–608.
- Solito E, et al. (2003) A novel calcium-dependent proapoptotic effect of annexin 1 on human neutrophils. *FASEB J* 17(11):1544–1546.
- Yao X, et al. (2006) Coupling ligand structure to specific conformational switches in the beta2-adrenoceptor. *Nat Chem Biol* 2(8):417–422.
- Boldt K, Rist W, Weiss SM, Weith A, Lenter MC (2006) FPRL-1 induces modifications of migration-associated proteins in human neutrophils. *Proteomics* 6(17):4790–4799.
- Mymrikov EV, Seit-Nebi AS, Gusev NB (2011) Large potentials of small heat shock proteins. *Physiol Rev* 91(4):1123–1159.
- De AK, Kodys KM, Yeh BS, Miller-Graziano C (2000) Exaggerated human monocyte IL-10 concomitant to minimal TNF-alpha induction by heat-shock protein 27 (Hsp27) suggests Hsp27 is primarily an antiinflammatory stimulus. *J Immunol* 165(7): 3951–3958.
- Bozinovski S, et al. (2012) Serum amyloid A opposes lipoxin A₄ to mediate glucocorticoid refractory lung inflammation in chronic obstructive pulmonary disease. *Proc Natl Acad Sci USA* 109(3):935–940.
- Patel HB, et al. (2012) The impact of endogenous annexin A1 on glucocorticoid control of inflammatory arthritis. *Ann Rheum Dis* 71(11):1872–1880.
- Ferlazzo V, et al. (2003) Anti-inflammatory effects of annexin-1: Stimulation of IL-10 release and inhibition of nitric oxide synthesis. *Int Immunopharmacol* 3(10–11): 1363–1369.
- Souza DG, et al. (2007) The required role of endogenously produced lipoxin A₄ and annexin-1 for the production of IL-10 and inflammatory hypo-responsiveness in mice. *J Immunol* 179(12):8533–8543.
- Ortega-Gómez A, Perretti M, Soehnlein O (2013) Resolution of inflammation: An integrated view. *EMBO Mol Med* 5(5):661–674.
- Vago JP, et al. (2012) Annexin A1 modulates natural and glucocorticoid-induced resolution of inflammation by enhancing neutrophil apoptosis. *J Leukoc Biol* 92(2): 249–258.
- Duffin R, Leitch AE, Fox S, Haslett C, Rossi AG (2010) Targeting granulocyte apoptosis: Mechanisms, models, and therapies. *Immunol Rev* 236:28–40.
- Rossi AG, et al. (2006) Cyclin-dependent kinase inhibitors enhance the resolution of inflammation by promoting inflammatory cell apoptosis. *Nat Med* 12(9):1056–1064.
- Särndahl E, et al. (2010) Enhanced neutrophil expression of annexin-1 in coronary artery disease. *Metabolism* 59(3):433–440.
- Connolly M, et al. (2010) Acute serum amyloid A induces migration, angiogenesis, and inflammation in synovial cells in vitro and in a human rheumatoid arthritis/SCID mouse chimera model. *J Immunol* 184(11):6427–6437.
- Leoni G, et al. (2013) Annexin A1, formyl peptide receptor, and NOX1 orchestrate epithelial repair. *J Clin Invest* 123(1):443–454.
- Grond-Ginsbach C, et al. (2008) Gene expression in human peripheral blood mononuclear cells upon acute ischemic stroke. *J Neurosci* 28(5):723–731.
- Barnig C, et al. (2013) Lipoxin A₄ regulates natural killer cell and type 2 innate lymphoid cell activation in asthma. *Sci Transl Med* 5(174):174ra26.
- Bento AF, Claudino RF, Dutra RC, Marcon R, Calixto JB (2011) Omega-3 fatty acid-derived mediators 17(R)-hydroxy docosahexaenoic acid, aspirin-triggered resolvin D1 and resolvin D2 prevent experimental colitis in mice. *J Immunol* 187(4):1957–1969.
- Petasis NA, et al. (2008) Design and synthesis of benzo-lipoxin A4 analogs with enhanced stability and potent anti-inflammatory properties. *Bioorg Med Chem Lett* 18(4):1382–1387.
- Dalli J, et al. (2013) Pro-resolving and tissue protective actions of Annexin A1-based cleavage resistant peptides are mediated by FPR2/ALX. *J Immunol* 190(12):6478–6487.
- Kirpotina LN, et al. (2010) Identification of novel small-molecule agonists for human formyl peptide receptors and pharmacophore models of their recognition. *Mol Pharmacol* 77(2):159–170.

Supporting Information

Cooray et al. 10.1073/pnas.1308253110

SI Materials and Methods

Drugs, Reagents, and Antibodies. Agonists at the lipoxin A₄ (LXA₄) receptor termed ALX (also called formyl peptide receptor type 2 or FPR2) used were annexin A1 (a kind gift from Chris Reutelingsperger, Maastricht University, Maastricht, The Netherlands) and LXA₄ (EMD Chemicals). Complete physical validation of lipoxin A₄ was obtained with liquid chromatography-tandem mass spectrometry (LC-MS-MS) and UV matching those reported earlier (1, 2). Fig. S3 reports the MS-MS spectrum and diagnostic ions confirming the correct structure, the UV-conjugated tetraene chromatophore and chromatographic behavior, three key points for the matching of the material used in the present experiments. The concentration was determined by UV spectrometry using absorption at 301 nm (in methanol) and an extinction coefficient of 40,000. Peptide Ac-AMVSEFLKQAW-FIENEEQEYVQTVK (Ac2-26) was from Tocris, SAA from Peprotech, whereas compound 43 (Cpd43; a nitrosylated pyrazolone derivative with agonistic activity at ALX receptor) was a generous gift from Amgen (Thousand Oaks, CA). The ALX-specific antagonist WRW4 (EMD Chemicals) and the FPR1-specific antagonist cyclosporin H were purchased from Biomol. Angiotensin II was purchased from Sigma-Aldrich.

The p38 inhibitor SB203580 and the JNK inhibitor SP600125 were purchased from Cell Signaling Technologies. Anti-Flag M2, anti-Flag M1, and anti-HA7 antibodies were purchased from Sigma-Aldrich; anti-HA11 was purchased from Covance (supplied by Cambridge Bioscience); and Alexa secondary antibodies (488 and 594) were purchased from Life Technologies. Rabbit anti-GAPDH was purchased from Santa Cruz Biotechnology, and Hsp27 mouse mAb, rabbit phospho-heat shock protein-27 (Hsp27), rabbit MAPK-activating protein kinase (MAPKAPK)-2, phosphoMAPKAPK-2, MAPKAPK1, phosphoMAPKAPK1, p38, phospho-p38, JNK, phospho-JNK, caspase 3, ERK, and phospho-ERK antibodies were purchased from Cell Signaling Technology. Moesin and phospho-Moesin antibodies were purchased from Abcam. Anti-Flag agarose beads and anti-HA agarose beads were purchased from Sigma-Aldrich.

Plasmid Constructions, Cell Culture, and Transfections. FPR1-Renilla luciferase (Rluc), ALX-Rluc, and FPR3-Rluc were generated by subcloning human FPR1, ALX, and FPR3 into the codon humanized *Renilla* luciferase vectors pRLuc-N1 and pRLuc-C3 (Perkin-Elmer). FPR1-enhanced yellow fluorescent protein (EYFP) and ALX-EYFP were generated by cloning FPR1 and ALX into the expression vectors pEYFP-N1 and -C1 (Clontech). AT1R-EYFP was generated by subcloning angiotensin II receptor type 1 (AT1R) into pEYFP-N1. β -arrestin-Rluc was generated by cloning β -arrestin2 into pEYFP-N1 and replacing EYFP with Rluc (3). FPR1 \times 3Flag and ALX \times 3Flag constructs were generated by subcloning human FPR1 and ALX into the p3 \times Flag-CMV-14 vector (Sigma-Aldrich). The FPR1 \times 3HA, ALX \times 3HA, and FPR3 \times 3HA constructs were obtained from Missouri S&T cDNA Resource Center (www.cDNA.org). HEK293A cells were maintained in DMEM containing 10% FCS and 1% penicillin/streptomycin. Cells were transfected with Lipofectamine 2000 (Invitrogen). The U937 monocyte cell line was maintained in RPMI 1640 supplemented with 10% FCS, 1% l-glutamine, 1% nonessential amino acids, and 1% penicillin/streptomycin. Cells were kept at 37 °C with 5% CO₂.

Reverse Transcriptase PCR. Total RNA was extracted from HEK293 cells and U937 cells. cDNA was synthesized and then used for PCR

analysis using the following ALX-specific primer pair: (5' to 3') TTG GTT TCC CTT TCA ACT GG as the sense primer and (5' to 3') AGA CGT AAA GCA TGG GGT TG as the antisense primer.

Fluorescence-Associated Cell Sorting and Confocal Microscopy Analyses. HEK293 cells were transfected with \times 3HA-tagged FPRs; 24-h posttransfection cell surface expression of receptors was determined using 1:100 dilution of anti-HA antibodies (Sigma-Aldrich). A final staining with anti-rabbit IgG was conducted. Flow cytometry analysis was performed by analyzing 10,000 events using a FACS Calibur flow cytometer (BD Biosciences) equipped with CellQuest software (BD Biosciences), followed by analysis using FlowJo (version 9.2, TreeStar). Results are reported as median fluorescence intensity units.

For receptor colocalization studies, cells were cotransfected with HA-tagged FPR1 and FLAG-tagged ALX and replated onto gelatin-coated 18-mm glass coverslips. Twenty-four hours later, live cells were incubated with anti-FLAG M1 antibody and anti-HA antibody (Sigma) directed against the N-terminal tags (1:1,000, 30 min). Cells were then fixed with 4% formaldehyde in PBS for 15 min, washed three times in 50 mM Tris base pH 7.4, 150 mM NaCl, 1 mM CaCl₂, and blocked and permeabilized in blocking buffer (0.1% Triton X-100, 3% milk, 1 mM CaCl₂, and 50 mM Tris-HCl, pH 7.4). Next, cells were stained with fluorescently conjugated secondary antibody (Alexa 488/594 1:500; Invitrogen). Coverslips were mounted using vectastain (Vector Laboratories) containing DAPI and visualized using a Zeiss LSM confocal microscope.

BRET Assay in Living Cells. HEK293 cells were transiently transfected as described above. The donor:acceptor ratio was varied for optimization of BRET conditions and the optimum ratio of 1:1 was used for subsequent transfections. Expression levels of the donor and acceptor constructs were determined using fluorescence microscopy and luminometry. Twenty-four hours posttransfection, cells were washed and transferred into 96-well black optiplates (Perkin-Elmer) using Hepes-buffered Ham's F-12 media (Sigma-Aldrich). For end-point assays, 24 h after transfection, cells were stimulated with ligands for 10 min. Coelenterazine-h (Invitrogen) was added in Hepes-buffered Ham's F-12 to a final concentration of 5 μ M and readings were collected immediately following this addition using the Polarstar Omega plate reader (BMG Labtech) that allows simultaneous dual-emission detection. For real-time experiments coelenterazine-h was added to a final concentration of 5 μ M directly before ligand injection. Readings were taken immediately at 0.2-s intervals for 40 s followed by 3-s intervals for 160 s and 60 s intervals for 700 s. Cells were kept at 37 °C throughout the BRET measurements. The BRET ratio is defined as emission at 530 nm (light emitted by EYFP)/emission at 485 nm (light emitted by Rluc). The normalized BRET ratio was calculated by subtracting the BRET ratio obtained in cells expressing the donor only (Rluc) from cells coexpressing both donor (Rluc) and acceptor (EYFP)-tagged constructs, as described before (3).

Proteome Profiler Arrays. FPR1, ALX, or FPR1 + ALX-transfected HEK293 cells were stimulated with agonist as per experimental design. Typically, we used AnxA1 (10⁻⁸ M), SAA (10⁻⁷ M), or peptide Ac2-26 (10⁻⁵ M) with an incubation time of 10 min, using resting cells as control. Lysates were prepared and protein quantification carried out using the Bio-Rad protein assay (Bio-Rad Laboratories) according to the manufacturer's instruction. Each sample was then used for the human phospho-MAPK array kit (R&D Systems) used according to the manufacturer's instructions.

Briefly, cell lysates (200 µg) were deposited on nitrocellulose membranes, spotted in duplicate with capture and control antibodies. A phospho site-specific biotinylated antibody mixture was used to detect phosphorylated kinases. The arrays were exposed to streptavidin-HRP and the ECL detection system before development on X-ray films. Spots were identified by alignment with the grid provided in the kit.

Isolation of Human Primary Neutrophils and Monocytes. All volunteers gave informed consent to blood collection and cell separation, as per the City and the East Ethics Committee (reference 05/Q0603/34, London). Peripheral blood from healthy donors was collected by i.v. withdrawal in 3.2% (wt/vol) sodium citrate solution (1:10). Polymorphonuclear leukocytes were isolated from blood via density centrifugation on a Histopaque 1119/1077 gradient (Sigma-Aldrich) according to the manufacturer's instructions and suspended in PBS + 0.5% BSA. Human primary monocytes were separated using the RosetteSep cell isolation kit (Stem Cell Technologies) according to manufacturer instructions.

Western Blotting and Coimmunoprecipitations. Western blotting was carried out using transfected HEK293 cells, U937 monocytes, human primary monocytes, or neutrophils. For dimerization studies, HEK293 cells were transfected with FPR1 × 3Flag, ALX × 3HA, and/or FPR1 × 3HA, ALX × 3HA or FPR3 × 3HA constructs and, 24 h later, stimulated for 10 min with the agonists. Cells were scraped into lysis buffer containing PBS + 0.1% n-dodecyl-β maltoside and a protease inhibitor mixture. For coimmunoprecipitations (co-IPs), the lysates were incubated with anti-hemagglutinin (HA) agarose beads and incubated at room temperature for another 2 h. SDS loading buffer was added to the samples and subjected to Western blotting using a 1:1,000 dilution of the anti-Flag antibody M2. Secondary antibody IRDye 800CW goat anti-mouse IgG (LI-COR Biotechnology) was used at a 1:10,000 dilution and imaged using the LI-COR Odyssey Infrared Image system. The protein marker used was a Full-Range Rainbow Molecular Weight Marker (GE Healthcare).

IL-10 Production from Human Monocytes. Isolated human monocytes (1×10^6) were incubated in 250 µL medium in round-bottomed 96-well plates at 37 °C, in a 5% CO₂ atmosphere. In some cases,

AnxA1 was added at 10^{-8} M, before or after pretreatment for 10 min at 37 °C with the p38 inhibitor SB203580 (10^{-7} M; Sigma-Aldrich). After a 6-h incubation, cell-free supernatants were harvested and used to quantify human IL-10 levels with a specific ELISA (eBioscience), using the manufacturer's instructions.

Assessment of Apoptosis. Freshly prepared neutrophils were treated with SAA (10 µg/mL) in the presence or absence of the JNK inhibitor SP600125 (20 µM; Calbiochem) after a 30-min preincubation with Ac2-26 ($0-10^{-5}$ M). Cells were then incubated for an additional 6, 12, or 24 h at 37 °C in a 5% CO₂ atmosphere. Neutrophils were stained with FITC-AnxAV and propidium iodide (PI) using the apoptosis detection kit from BD Pharmingen, following manufacturer instructions, and analyzed by flow cytometry (BD FACSCalibur).

Animal Experiments. Animals were used according to the guidelines of the Queen Mary University of London Ethical Committee for the Use of Animals. Animal work was performed according to Home Office Regulations (Guidance on the Operation of Animals, Scientific Procedures Act, 1986). Male C57BL/6 (Charles River) and Alx-Fpr2/3 KO (4) mice (20–25 g body weight) were used. Mice were maintained on a standard chow pellet diet with tap water ad libitum. In the first set of experiments, mice were treated i.p. with human recombinant AnxA1 (1 µg) or saline. Peritoneal cavities were washed 6 h later with 3 mL of PBS, containing 3 mmol/L ethylenediamine tetraacetic acid. In a second set of experiments, mice were injected with 10 mg/kg i.p. of *Escherichia coli* LPS (serotype 0111:B4, specific activity, >500,000 units/mg) and peritoneal cavity was washed, and the contents were collected from 6 to 24 h later. IL-10 was measured in peritoneal lavages by the murine Ready-Set-Go ELISA kit according to the manufacturer's instructions (eBioscience). Mouse AnxA1 was measured by an in-house ELISA.

Statistical Analysis. The data reported are the mean ± SEM of at least three independent experiments, each performed at least in duplicate. Statistical analysis was performed using one-way ANOVA or, in the case of apoptosis in primary cells, two-way ANOVA, taking a *P* value less than 0.05 as significant.

1. Serhan CN, Hamberg M, Samuelsson B (1984) Trihydroxytetraenes: A novel series of compounds formed from arachidonic acid in human leukocytes. *Biochem Biophys Res Commun* 118(3):943–949.
2. Clish CB, Levy BD, Chiang N, Tai HH, Serhan CN (2000) Oxidoreductases in lipoxin A4 metabolic inactivation: A novel role for 15-*o*-prostaglandin 13-reductase/leukotriene B4 12-hydroxydehydrogenase in inflammation. *J Biol Chem* 275(33):25372–25380.

3. Cooray SN, Chung TT, Mazhar K, Szidonya L, Clark AJ (2011) Bioluminescence resonance energy transfer reveals the adrenocorticotropin (ACTH)-induced conformational change of the activated ACTH receptor complex in living cells. *Endocrinology* 152(2):495–502.
4. Duffon N, et al. (2010) Anti-inflammatory role of the murine formyl-peptide receptor 2: Ligand-specific effects on leukocyte responses and experimental inflammation. *J Immunol* 184(5):2611–2619.

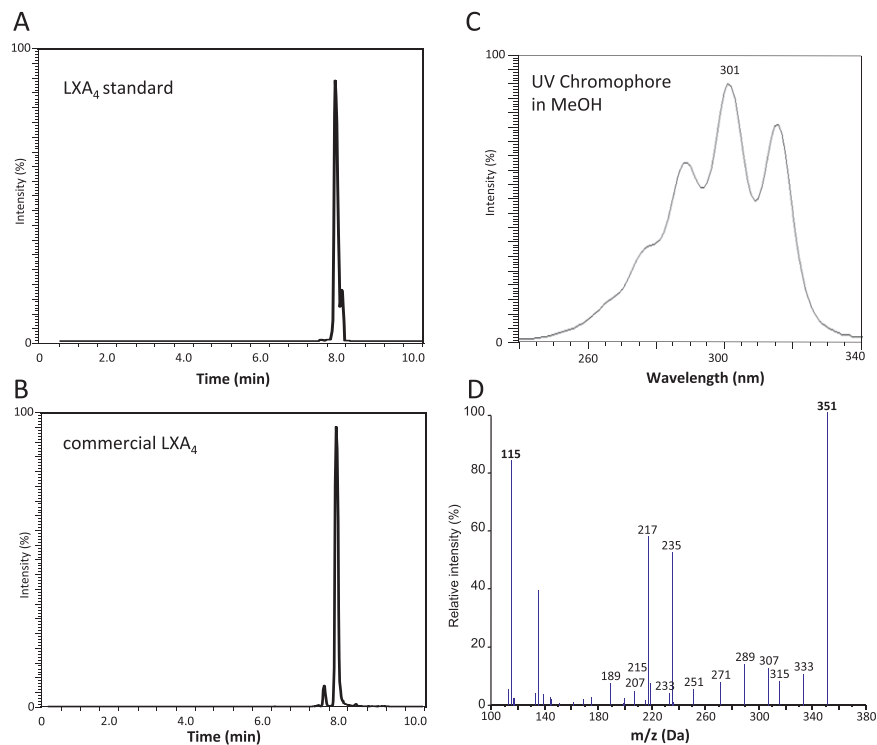


Fig. S3. Validation of the LXA₄ used in the BRET experiments. (A) High-pressure liquid chromatography (HPLC) trace for LXA₄ standard. (B) HPLC trace, (C) UV spectrum, and (D) MS-MS spectrum for commercially sourced LXA₄ used in this study. The MS-MS spectrum with diagnostic ions, the UV-conjugated tetraene chromophore, and chromatographic behavior are three key points confirming the correct structure of lipoxin A₄ used in the present experiments.

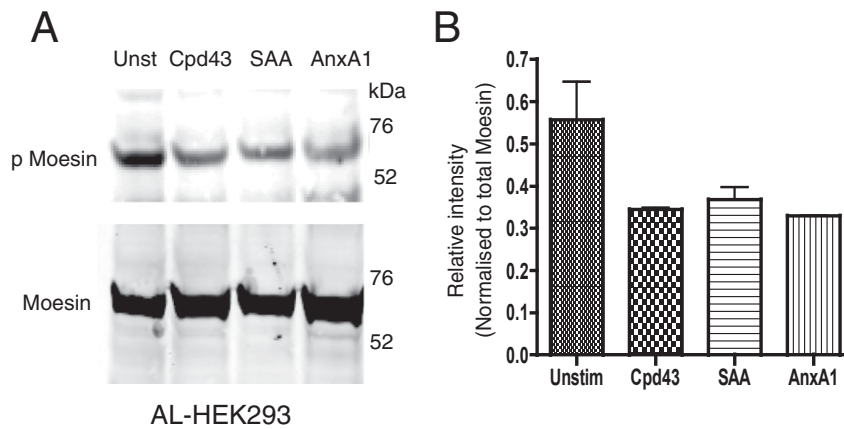


Fig. 55. ALX receptor-mediated signaling in response to its anti-inflammatory agonists AnxA1 and compound 43 and proinflammatory agonist SAA. (A) Phosphorylation status of Moesin. HEK293 cells were transfected with ALX receptor and stimulated with compound 43 (10^{-6} M), SAA (10^{-7} M), and AnxA1 (10^{-8} M) for 10 min. Lysates were subjected to Western blotting analysis using antibodies against the phosphorylated or unphosphorylated Moesin [phospho-Moesin (pMoesin) or Moesin antibody, which also detects Radixin]. (B) Densitometry analysis of three independent Western blot experiments.

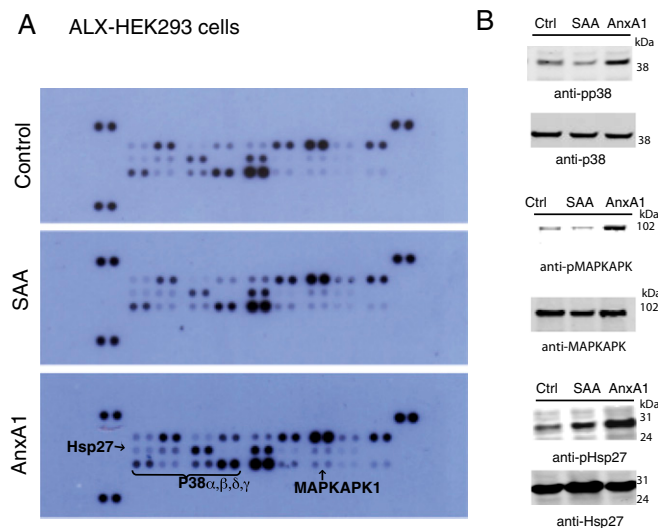


Fig. 56. Identification of ALX/ALX proresolving signaling signature. (A) Proteome profiler array on ALX-transfected HEK293 cells stimulated with AnxA1 (10^{-8} M) or SAA (10^{-7} M) for 10 min (see *Materials and Methods* for details). (B) Western blotting analyses to detect the phosphorylation status of p38, MAPKAPK, and Hsp27 in ALX-HEK293 cells. Cells (1×10^6) were treated for 10 min with vehicle (Ctrl), AnxA1 (10^{-8} M), or SAA (10^{-7} M) and lysates subjected to Western blotting and probed with antibodies against phosphorylated and unphosphorylated p38, MAPKAPK, and Hsp27.

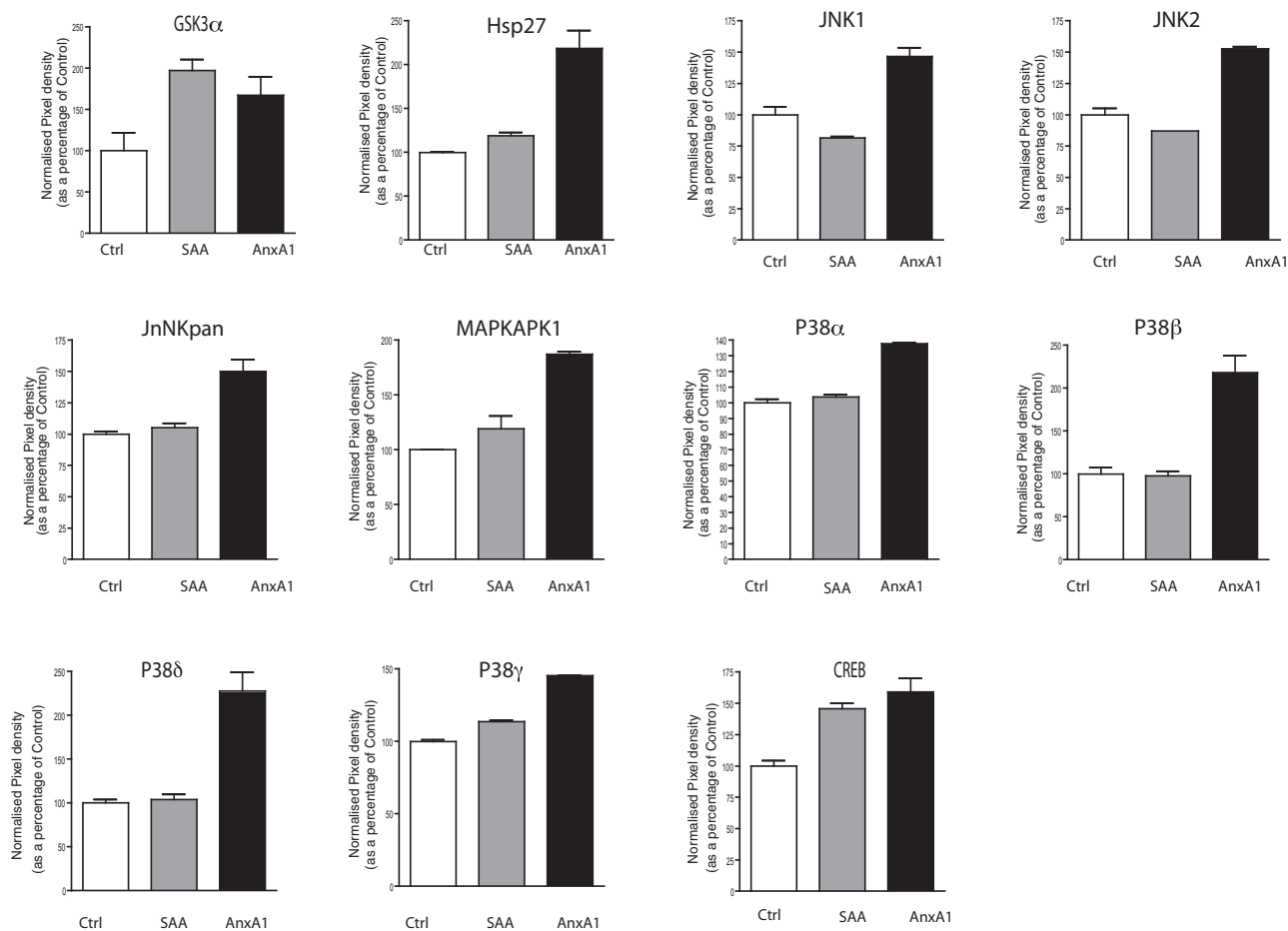


Fig. S7. Densitometric analysis of phosphorylation states of a number of serine/threonine kinases in ALX-transfected HEK293 cells as shown in Fig. S5. Results are expressed in arbitrary units of densitometry.

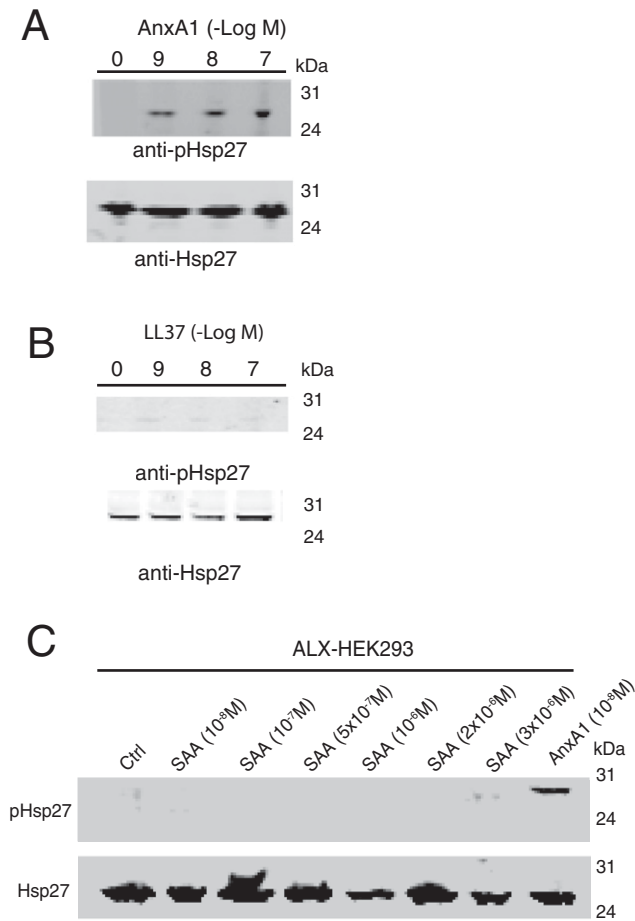


Fig. 58. Concentration–response profiles of phospho-Hsp27 in ALX-HEK293 cells stimulated for 10 min with the reported concentrations of (A) AnxA1, (B) LL-37, or (C) SAA.

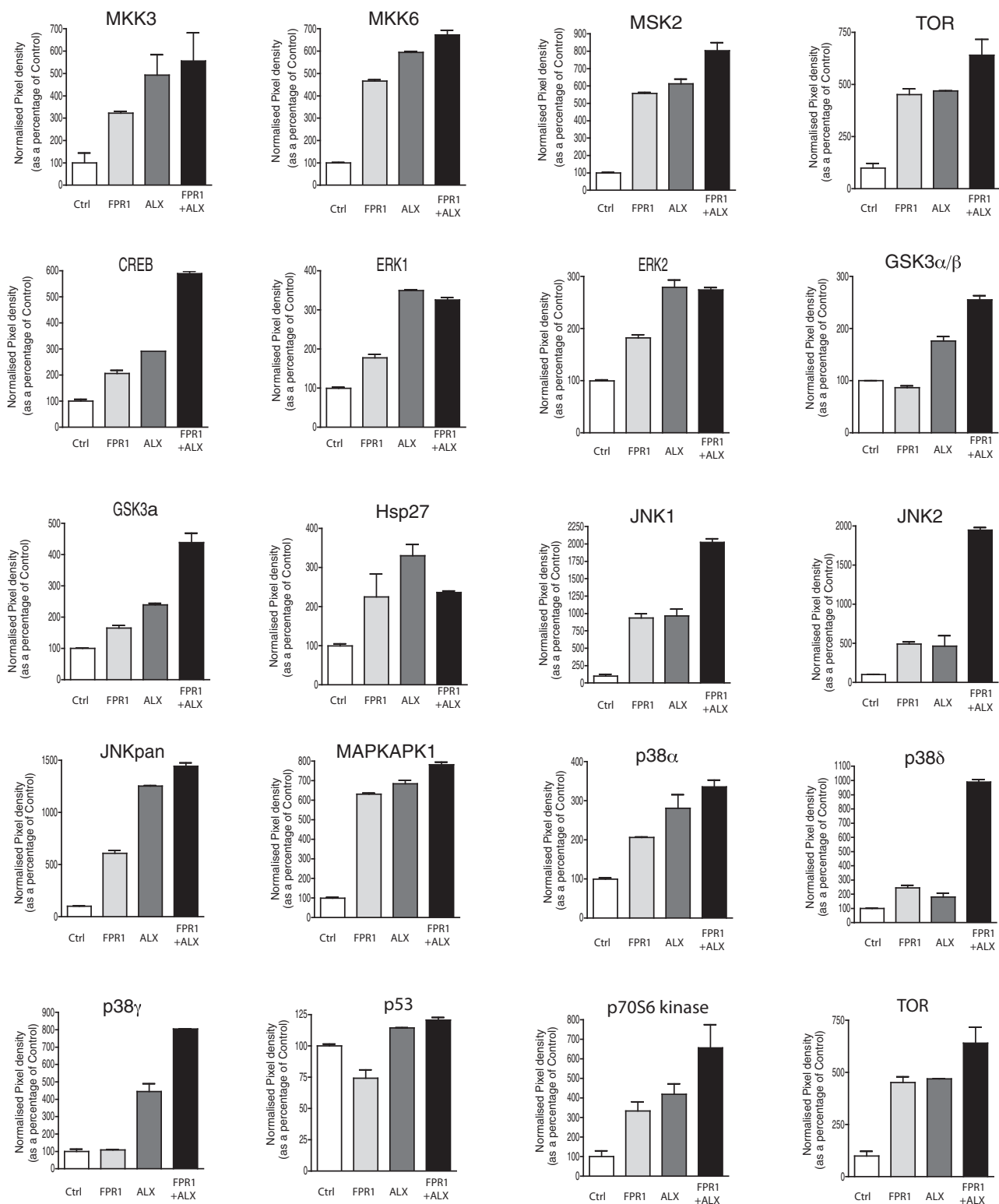


Fig. 59. Densitometric analysis of phosphorylation states of serine/threonine kinases in FPR1, ALX, and FPR1 + ALX-transfected HEK293 cells treated with Ac2-26 (10^{-5} M) for 10 min; see Fig. 4 for correspondent profiler. Results are expressed in arbitrary units of densitometry.